Investigations into nanofluids as direct solar radiation collectors

Elsevier Editorial System(tm) for Solar Energy

Manuscript Draft

Manuscript Number: SE-D-16-01573R2

Title: Investigations into nanofluids as direct solar radiation collectors

Article Type: Research paper

Section/Category: Solar heating & cooling, buildings, and other applications

Keywords: Nanofluid,
Direct solar absorption,
Solar thermal collector,
Optical absorption,
Nanofluid stability,
Wave optics model

Corresponding Author: Dr. H. Singh, Ph.D.

Corresponding Author's Institution: Brunel University

First Author: B.A.J. Rose

Order of Authors: B.A.J. Rose; H. Singh, Ph.D.; N. Verma; S. Tassou; S. Suresh; N. Anantharaman; D. Mariotti; P. Maguire

Abstract: Nanofluids that directly absorb solar radiation have been proposed as an alternative to selectively coated metallic receivers in solar thermal collectors. Given the expense of characterising a potential nanofluid experimentally methods for comparing nanofluids virtually are needed. This paper develops a computational wave optics model using COMSOL to simulate the absorption of nanoparticles suspended in a fluid for solar radiation (380-800 nm) and compares it to experimental results using reflectance and transmission spectrometry. It was concluded that while both yielded data with matching trends, the exact absorption of some fluids differed by up to 1 AU. Optical characteristics of nanofluids comprising ethylene glycol (melting point -12.99 °C and boiling point range 195 - 198 °C at 1,013 hPa) and graphene oxide (sheets size 5nm x 19nm x 19nm, volume fraction 0.004-0.016%) have been experimentally measured. An optimum volume fraction of 0.012% of graphene oxide has been identified achieving a minimum reflectance and highest absorbance over the visible spectral range.

Suggested Reviewers: Prashant Dhiman PhD
Associate Professor , Ntonal Institute of Technology Hamirpur Indian
prashant_rec@yahoo.co.in
expertise and experience in solar thermal energy systems and technologies

Tariq Muneer Phd
Professor, Edinburgh Napier University
T.Muneer@Napier.ac.uk
Relevant experience of several years of research into solar energy technologies

David Redpath PhD
drdredpath@gmail.com
Expert in low temperature solar energy systems

Response to Reviewers: Response to Reviewers

Reviewer #2:
Query 1: A justification for the geometrical distribution that was chosen (e.g. why this lattice was used instead of a more regular or more complex one);
Response: Assumptions are described in the sections 2.1 and 3.1. Nevertheless, the justifications that we provide for our geometrical distribution are as follows:
1. Page 5 (line 5-7): The control volume was large enough to avoid effects resulting from scales close to those of the wavelengths used (diffraction off the edges of the volume) and yet small enough to compute reasonably fast (around 1 hour).
2. Page 5 (line 23-28): Within the control volume two arrays were defined comprising identical 5nm x 19nm x 19nm nanoplatelets making up the equivalent of 0.1% of the simulated volume.--------- The arrays were positioned off set from each other so the distance between each particle and a neighbouring particles was not the same, in all directions, see figure 1. This was done to simulate a realistic nanofluid in which the nanoparticles will be randomly distributed.
3. Control volume simulated had a square cross-section of 1x1 µm, see fig. 1.
4. Page 7 (lines 6-9) : Near the edges of the control volume the boundary conditions force the electric field to be close to zero, as a result smaller control volumes were not penetrated by the electric field. In figure 2 the volume has a cross section measuring 1 µm x 1 µm, which is sufficiently large for the electric field in the centre to propagate mostly unaffected by the boundaries.

Query 2: Specify if the model is allowing for the presence local clusters or not;
Response: No, the current model did not assume any clusters, though it can be modified to simulate them.

Query 3: describe the type of interactions (if any) between the nanoplatelets;
Response: The model did not explicitly consider any physical interactions between nanoplatelets, but the effect of the nanoparticles' arrangement in the array was observed as is evident from Fig 2 and 3. However, the nanofluids were experimentally characterised allowing interactions among nanoplatelets.

Query 4: How the change in concentration and shape will affect the various parameters etc.
Response: We have conducted experimental measurements and computer modelling a for range of volume fractions of 0.004%, 0.008%, 0.012%, 0.013%, 0.014% and 0.016% (Page 5, line --)' and the results are indicated in fig 7-9. However, the effect of shape has not been considered. This will be performed in a follow up study, which is under progress these days.

Query 4: In the present form, the described methodology only allows the reader to deduce some of these assumptions based on the results, but it is not clear whether or not those assumptions were actually considered to begin with.
Response: I can confirm all the assumptions mentioned at different locations in the paper have been adopted by the model.

Query 5: Page 5 Line 17-18 Remove "and as such a 10m length of copper will have the same electrical conductivity as 10cm" as the statement is clear.
Response: As suggested, this change has been done.

Query 6: Page 5 Line 56-57 A "critical concentration at which the nanoparticles start to bundle" is mentioned, but its actual value is not provided. There are cases reported in the literature where the graphene "nanoparticles" can start to bundle at a concentration of 0.01%. Thus, this can also raise questions on the stability measurement as this was monitored at a lower concentration (0.008%). So, its value should be mentioned to avoid confusions. Also, the text should be consistent in using the terms nanoplatelets and nanoparticles i.e. use only one.

Response: (i) In this work, we did not evaluate the critical concentration to avoid bundling of nanoparticles. As described in sections 2.2.3 and 3.2.3, our main intention was check the suspension's stability over the likely period of idleness (24 hrs) relevant to solar energy plants. No bundling was observed during this duration for the concentration of 0.008% investigated in our study.
(ii) We have replaced the term nanoplatelet with nanoparticle throughout the document.
Query 6: Page 7-8 and Figure 2 – 5 and 7
The electric field variation will be influenced by the concentration and shape of the graphene. However, for figure 2 and 3 the parameters for which those were obtained are not specified in clear. While Figure 2 can be considered as a typical distribution of the electric field in 2D (the geometry was defined in 3D!!!), Figure 3 should show the variation of the electric field with depth (including the trend lines) for the various concentrations (e.g. 0.004, 0.008 and 0.012%) and shape (cuboid and spherical). This will provide the reader with a better understanding of the model and the implications of modifying the distance between particles (i.e. of the concentration) and the shape (described in Figure 4). If the figure becomes too populated then these dependencies can be presented in different figures. Also, in caption of the Figure 2, the parameters for which this modelling was performed should be included.
Figure 5 presents the modelled values of the absorbance, but this information is repeated in Figure 7. I will suggest removing figure 5 and keep only the Figure 7, but the absorbance for graphene oxide should be included. Thus, a new figure 7 should be made and it should contain the following information:
-the modelled data using graphene and the corresponding trendline
-the modelled data using graphene oxide and the corresponding trendline
-the experimental data with error bars (at the present no error bars are present) and the corresponding trendline
Response: (i) The nanoparticles in the simulated volume were assigned the complex refractive index of Graphene sheets 2.0-1.1i. The control volume has a cross section measuring 1 µm x 1 µm and a length of 8 µm. The size of the control volume, nanoparticle size and distribution (concentration) was adopted to avoid effects resulting from scales close to those of the wavelengths used (diffraction off the edges of the volume) and yet small

enough to compute reasonably fast (around 1 hour). The parameters relevant for figure 2, 3 are described in sections 2.1 and 3.1.
(ii) We did not include the modelling parameters in the caption of figure 2 to avoid repetition.
(iii) Figure 5 shows the model results for graphene and ethylene glycol based nonofluids, whereas figure six experimental results for graphene oxide nanoparticles based nanofluids. For clarity, we would like to keep the figures separate as they are now.
(iii) Figure 7, error bars have been added to the measured values shown.

Query 6: Page 7 Line 51-52
The message of the sentence is not very clear. Please rephrase.
Response: Although we will be happy to alter or rephrase the sentences, we are not able to identify exactly which line is being mentioned in this comment.
Query 7: Page 8 and Figure 9
The stability is demonstrated by providing the absorbance for various wavelengths in time only for the 0.008%. However, to prove the stability for the other samples, one can show the variation of the absorbance for all concentrations. This can be done by describing the time variation of the absorbance at one (or more, if needed) wavelength(s) e.g. 555 nm for all the concentrations studied.
Response: Due to limited time and resources available we could not measure absorbance for each sample to ascertain their stability. However, in future we will be doing this and report accordingly in a follow up paper.

Query 8: In the 4th Editor comment, the possibility of implementing this model in the real applications is mentioned. The authors are responding that this analysis was performed based on a UK typical building, but no data are included to sustain it. This will be important as the main claim of the manuscript is that the wave optics model can provide an alternative tool for designing new nanofluids and it can reduce the need of extensive and expensive lab trials.
Response: We regret that our previous response was confusing. We did not consider any specific location or type of building for this analysis. Our work focusses on understanding the behaviour of nano-suspensions for use as working fluid in direct solar absorption type solar collectors. Such collectors can be implemented onto buildings or in the large ground mounted concentrating solar thermal or power plants. These offer opportunity to develop alternative (cheaper) and simpler designs due to the scope of miniaturisation. In this regard, the present work is an important step as it shows how wave-optics model can be used to replace expensive and time consuming experiments to design and size the solar field using volumetrically absorbing solar collectors.

Response to Reviewers

Reviewer #2:

Query 1: *A justification for the geometrical distribution that was chosen (e.g. why this lattice was used instead of a more regular or more complex one);*
Response: Assumptions are described in the sections 2.1 and 3.1. Nevertheless, the justifications that we provide for our geometrical distribution are as follows:

1. Page 5 (line 5-7): The control volume was large enough to avoid effects resulting from scales close to those of the wavelengths used (diffraction off the edges of the volume) and yet small enough to compute reasonably fast (around 1 hour).
2. Page 5 (line 23-28): Within the control volume two arrays were defined comprising identical 5nm x 19nm x 19nm nanoplatelets making up the equivalent of 0.1% of the simulated volume.--------- The arrays were positioned off set from each other so the distance between each particle and a neighbouring particles was not the same, in all directions, see figure 1. This was done to simulate a realistic nanofluid in which the nanoparticles will be randomly distributed.
3. Control volume simulated had a square cross-section of 1x1 µm, see fig. 1.
4. Page 7 (lines 6-9) : Near the edges of the control volume the boundary conditions force the electric field to be close to zero, as a result smaller control volumes were not penetrated by the electric field. In figure 2 the volume has a cross section measuring 1 µm x 1 µm, which is sufficiently large for the electric field in the centre to propagate mostly unaffected by the boundaries.

Query 2: *Specify if the model is allowing for the presence local clusters or not;*
Response: No, the current model did not assume any clusters, though it can be modified to simulate them.

Query 3: *describe the type of interactions (if any) between the nanoplatelets;*
Response: The model did not explicitly consider any physical interactions between **nanoplatelets**, but the effect of the nanoparticles' arrangement in the array was observed as is evident from Fig 2 and 3. However, the nanofluids were experimentally characterised allowing interactions among nanoplatelets.

Query 4: *How the change in concentration and shape will affect the various parameters etc.*
Response: We have conducted experimental measurements and computer modelling a for range of volume fractions of 0.004%, 0.008%, 0.012%, 0.013%, 0.014% and 0.016% (Page 5, line --)' and the results are indicated in fig 7-9. However, the effect of shape has not been considered. This will be performed in a follow up study, which is under progress these days.

Query 4: *In the present form, the described methodology only allows the reader to deduce some of these assumptions based on the results, but it is not clear whether or not those assumptions were actually considered to begin with.*
Response: I can confirm all the assumptions mentioned at different locations in the paper have been adopted by the model.

Query 5: *Page 5 Line 17-18 Remove "and as such a 10m length of copper will have the same electrical conductivity as 10cm" as the statement is clear.*
Response: As suggested, this change has been done.

Query 6: *Page 5 Line 56-57 A "critical concentration at which the nanoparticles start to bundle" is mentioned, but its actual value is not provided. There are cases reported in the literature where the graphene "nanoparticles" can start to bundle at a concentration of 0.01%. Thus, this can also raise questions on the stability measurement as this was monitored at a lower concentration (0.008%). So, its value should be mentioned to avoid confusions. Also, the text should be consistent in using the terms nanoplatelets and nanoparticles i.e. use only one.*

Response: (i) In this work, we did not evaluate the critical concentration to avoid bundling of nanoparticles. As described in sections 2.2.3 and 3.2.3, our main intention was check the suspension's stability over the likely period of idleness (24 hrs) relevant to solar energy plants. No bundling was observed during this duration for the concentration of 0.008% investigated in our study.

(ii) We have replaced the term nanoplatelet with nanoparticle throughout the document.

Query 6: *Page 7-8 and Figure 2 – 5 and 7*
The electric field variation will be influenced by the concentration and shape of the graphene. However, for figure 2 and 3 the parameters for which those were obtained are not specified in clear. While Figure 2 can be considered as a typical distribution of the electric field in 2D (the geometry was defined in 3D!!!), Figure 3 should show the variation of the electric field with depth (including the trend lines) for the various concentrations (e.g. 0.004, 0.008 and 0.012%) and shape (cuboid and spherical). This will provide the reader with a better understanding of the model and the implications of modifying the distance between particles (i.e. of the concentration) and the shape (described in Figure 4). If the figure becomes too populated then these dependencies can be presented in different figures. Also, in caption of the Figure 2, the parameters for which this modelling was performed should be included.
Figure 5 presents the modelled values of the absorbance, but this information is repeated in Figure 7. I will suggest removing figure 5 and keep only the Figure 7, but the absorbance for graphene oxide should be included. Thus, a new figure 7 should be made and it should contain the following information:
-the modelled data using graphene and the corresponding trendline
-the modelled data using graphene oxide and the corresponding trendline
-the experimental data with error bars (at the present no error bars are present) and the corresponding trendline

Response: (i) The nanoparticles in the simulated volume were assigned the complex refractive index of Graphene sheets 2.0-1.1i. The control volume has a cross section measuring 1 µm x 1 µm and a length of 8 µm. The size of the control volume, nanoparticle size and distribution (concentration) was adopted to avoid effects resulting from scales close to those of the wavelengths used (diffraction off the edges of the volume) and yet small

enough to compute reasonably fast (around 1 hour). The parameters relevant for figure 2, 3 are described in sections 2.1 and 3.1.

(ii) We did not include the modelling parameters in the caption of figure 2 to avoid repetition.

(iii) Figure 5 shows the model results for graphene and ethylene glycol based nonofluids, whereas figure six experimental results for graphene oxide nanoparticles based nanofluids. For clarity, we would like to keep the figures separate as they are now.

(iii) Figure 7, error bars have been added to the measured values shown.

Query 6: Page 7 Line 51-52
The message of the sentence is not very clear. Please rephrase.
Response: Although we will be happy to alter or rephrase the sentences, we are not able to identify exactly which line is being mentioned in this comment.

Query 7: Page 8 and Figure 9
The stability is demonstrated by providing the absorbance for various wavelengths in time only for the 0.008%. However, to prove the stability for the other samples, one can show the variation of the absorbance for all concentrations. This can be done by describing the time variation of the absorbance at one (or more, if needed) wavelength(s) e.g. 555 nm for all the concentrations studied.
Response: Due to limited time and resources available we could not measure absorbance for each sample to ascertain their stability. However, in future we will be doing this and report accordingly in a follow up paper.

Query 8: In the 4th Editor comment, the possibility of implementing this model in the real applications is mentioned. The authors are responding that this analysis was performed based on a UK typical building, but no data are included to sustain it. This will be important as the main claim of the manuscript is that the wave optics model can provide an alternative tool for designing new nanofluids and it can reduce the need of extensive and expensive lab trials.

Response: We regret that our previous response was confusing. We did not consider any specific location or type of building for this analysis. Our work focusses on understanding the behaviour of nano-suspensions for use as working fluid in direct solar absorption type solar collectors. Such collectors can be implemented onto buildings or in the large ground mounted concentrating solar thermal or power plants. These offer opportunity to develop alternative (cheaper) and simpler designs due to the scope of miniaturisation. In this regard, the present work is an important step as it shows how wave-optics model can be used to replace expensive and time consuming experiments to design and size the solar field using volumetrically absorbing solar collectors.

Investigations into nanofluids as direct solar radiation collectors

B.A.J. Rose[a] , H. Singh[a*] , N. Verma[a], S. Tassou[a], S. Suresh[b], N. Anantharaman[b], D. Mariotti[c] , P. Maguire[c]

[a]Institute of Energy Futures, Brunel University London, Uxbridge, UB8 3PH, UK
[b]National Institute of Technology, Tiruchirappalli-620015, India
[c]Nanotechnology & Integrated Bio-Engineering Centre, Ulster University, Newtownabbey, BT37 0QB, UK

*Corresponding author (harjit.singh@brunel.ac.uk)

Abstract

Nanofluids that directly absorb solar radiation have been proposed as an alternative to selectively coated metallic receivers in solar thermal collectors. Given the expense of characterising a potential nanofluid experimentally methods for comparing nanofluids virtually are needed. This paper develops a computational wave optics model using COMSOL to simulate the absorption of nanoparticles suspended in a fluid for solar radiation (380-800 nm) and compares it to experimental results using reflectance and transmission spectrometry. It was concluded that while both yielded data with matching trends, the exact absorption of some fluids differed by up to 1 AU. Optical characteristics of nanofluids comprising ethylene glycol (melting point -12.99 °C and boiling point range 195 - 198 °C at 1,013 hPa) and graphene oxide (sheets size 5nm x 19nm x 19nm, volume fraction 0.004-0.016%) have been experimentally measured. An optimum volume fraction of 0.012% of graphene oxide has been identified achieving a minimum reflectance and highest absorbance over the visible spectral range.

Keywords: Nanofluid, Direct solar absorption, Solar thermal collector, Optical absorption, Nanofluid stability, Wave optics model

Highlights

- Different modelling approaches for the direct absorption of solar radiation by nanofluids discussed and evaluated.
- A wave optics model proposed for direct solar absorbing nanofluids.
- The wave optics model constructed and the results analysed.
- The optical properties of graphene oxide-ethylene glycol nanofluids characterised experimentally.
- The experimental results compared to those predicted by the model.

1. Introduction

Nanofluids, suspensions of nanoparticles in liquids, have been the focus of recent interest for use as directly absorbing working fluids, due to their reported stability in suspension and the availability of materials from which they can be synthesised (Romasanta et al., 2011). Directly absorbing nanofluids offer many advantages over traditional surface absorbers: reduced thermal and radiative

losses, potential for miniaturisation of solar concentrators and lower material costs (Toppin-Hector and Singh, 2013). The amount of solar radiation that a solar concentrator working fluid will directly absorb depends primarily on the type of fluid used and its solar absorption characteristics and the dimensions of the receiver tube (Gorji and Ranjbar, 2015; Toppin-Hector and Singh, 2013).

Extinction describes the reduction in the amount of radiation that is observed when any medium (gas or liquid or solid or a combination) is placed between a light source and a detector (Otanicar et al., 2009).

The attenuation of light intensity ($-dI_x$) as light passes through a layer of an absorbing medium is proportional to the intensity of light at the entrance of the medium layer (I_x) and the differential thickness of the layer (dx). Mathematically this relation can be expressed as (Maikala, 2010):

$$-dI_x = aI_x\, dx \tag{1}$$

Where

a is the wavelength dependent absorption or extinction coefficient

Equation (1) is popularly known as Bouguer-Lambert's law and in this equation '–' sign indicates a definite decrease in the intensity as light passes through any absorbing medium.

Previous studies have focussed on the scattering component using an adaptation of the Rayleigh approximation (Ladjevardi et al., 2013). However, the Rayleigh approximation only holds for particles that are spherical, are close in refractive index to the medium they are in, and are small in size relative to the wavelength (λ) such that $\ll \lambda/10$ (Kerker et al., 1978). Models based on the Rayleigh approximation will not be able to predict the optical properties of non-spherical particles such as graphene ~~nanoplatelets~~ nanoparticles.

Taylor et al. (2011) took a Maxwell-Garnett effective medium approach to model the optical properties of nanofluids based on the optical properties of the fluid and the bulk materials of the nanoparticles (NPs). Their study has a serious drawback in that they did not consider any difference in the electrical permittivity between a nano scale particle and a macro scale sample of the same metal. They concluded that the Maxwell-Garnett effective medium approach did not correctly predict the extinction caused by nanoparticles in a fluid but did not expand on the reason nor suggest alternative methods.

Beer-Lambert's law relates the reduction in the intensity of light with the depth of medium layer as it passes through an absorbing medium of a specific concentration (C). Thus equation (1) can be expressed as equation (2) as follows:

$$-dI_x = aI_xC\, dx \tag{2}$$

Equation (2) can be integrated over the thickness of the medium layer varying from $x = 0$ to $x = L$ to yield Beer's law (Maikala, 2010):

$$A = log_{10}\frac{I_o}{I} \tag{3}$$

Where

A is the absorbance of the absorbing medium

I_0 is the intensity of light that enters the medium

I is the intensity of light that leaves the medium layer of thickness L

Absorbance therefore can be easily linked with the depth of a medium. Beer-Lamberts law allows the absorbance for any path length through a medium to be calculated. This principle can be interpreted so that it is only necessary for a model to simulate the optical properties of a small volume of fluid to be useful for predicting the absorption of any volume. Currently the optical properties of each different fluid and particle combination must be measured experimentally to identify the ideal working fluid for a direct solar absorption application. If a computer model could be developed that is capable of identifying the most likely nanoparticle-fluid combinations, the process of designing a directly absorbing solar thermal concentrator would be greatly simplified.

1.1. Modelling approach

1.1.1. Raytracing

One of the simplest ways to model light absorption by objects is ray tracing. Ray tracing models light as being composed of several (how many depends on the precision of the model) infinitely narrow straight rays. A nanofluid would be simulated by a ray trace model as a series of opaque objects randomly distributed throughout a transparent medium (the population density and size of the objects is analogous to the volume fraction and size of nanoparticles). Rays are then passed through the virtual nanofluid and when they are incident on a nanoparticle they are considered to have been absorbed and propagate no further by simpler models. Once every incident ray has encountered a sphere and been absorbed, the distance travelled by the last ray to be absorbed and the number of rays used in the simulation can be used to estimate the depth of the fluid layer to cause full absorption of the solar radiation.

Ray trace models have the advantage of requiring relatively little information about the nanofluids and are based on simple geometric calculations to produce a result. However, they cannot accurately simulate the absorption of solar radiation by nanofluids as nanoparticles are significantly smaller than the wavelength of solar radiation.

The uncertainty in the position of a photon makes it difficult to determine if a photon will be absorbed by a nanoparticle using a ray trace model. For a photon, it can be derived from the uncertainty principle expressed in equation (4).

$$\Delta x \geq \frac{\lambda}{4\pi} \qquad (4)$$

where (Δx) is the uncertainty in position and (λ) is the wavelength.

For a photon of visible light uncertainty in the position is always greater than $\sim$40nm which is larger than the size of many nanoparticles considered for direct absorption (size $\sim 15-30$nm). As such modelling light as rays at scales less than this is not a meaningful analogy (Novotny, 2006). The wavelength of visible light could easily be around 10-25 times greater than the size of NPs. Thus, model assumption that light travels in straight lines and is only absorbed by particles on which it is directly incident is not valid (Bohen, 1983).

As a result of these two shortcomings, a purely ray tracing based model only considers the interaction between particles and light directly incident on it. Such a model would either under- or over-estimate the optical absorption by a nanofluid. An alternative would therefore be to simulate the process using ray tracing only at scales where its assumptions are sensible and an alternative model to simulate the fluid properties at smaller scales.

1.1.2. Wave optics

While the Rayleigh approximation was originally derived geometrically it has been shown to be consistent with wave optics (Bohren and Huffman, 1983).

The interaction of electric and magnetic fields is described physically by Maxwell's, equations (5)-(8).

$$\nabla \times \boldsymbol{E}(\boldsymbol{r},t) = -\frac{\partial \boldsymbol{B}(\boldsymbol{r},t)}{\partial t} \quad (5)$$

$$\nabla \times \boldsymbol{H}(\boldsymbol{r},t) = \frac{\partial \boldsymbol{D}(\boldsymbol{r},t)}{\partial t} + \boldsymbol{j}(\boldsymbol{r},t) \quad (6)$$

$$\nabla . \boldsymbol{D}(\boldsymbol{r},t) = \rho(\boldsymbol{r},t) \quad (7)$$

$$\nabla . \boldsymbol{B}(\boldsymbol{r},t) = 0 \quad (8)$$

Where (E) is the electric field; (D) is the electric displacement; (H) is the magnetic field; (B) is the magnetic induction; (j) is the current density, (ρ) is the charge density, $(\nabla \times)$ represents the curl of a vector and $(\nabla .)$ represents the divergence of the vector.

Light is therefore described by wave optics as an electromagnetic wave comprised of varying electric and magnetic fields orthogonal to each other and the direction of wave propagation.

In vacuum electromagnetic waves will continue to propagate indefinitely whereas in other mediums charges will be affected by the varying electrical and magnetic field which will diminish energy content of the wave as it passes through. In this way the electromagnetic wave is absorbed and its energy is transferred to the medium.

A medium's resistance to a change in electric field and magnetic field is given by the electrical permittivity (ε) and magnetic permeability (μ) respectively. These properties are more commonly represented in terms of the refractive index (n) (9).

$$n = \sqrt{\frac{\varepsilon}{\varepsilon_0}\frac{\mu}{\mu_0}} \quad (9)$$

Where (ε_0) is the electrical permittivity of free space and (μ_0) is the magnetic permeability of free space.

In most circumstances, at speeds much less than the speed of light or intensities less than 10^{18} W/m^2, only the electric field and electrical permittivity need be considered (Peatross, and Ware, 2011). The wave equation for the electric field in a medium with a refractive index (n) can be written as shown in equation (10).

$$\nabla^2 E - \frac{n^2}{c^2}\frac{\partial^2 E}{\partial t^2} = 0 \quad (10)$$

Where (c) is the speed of light.

A wave optics model of a nanofluid can be built from the refractive indices of the nanoparticles and base fluid, particle size and particle distribution in the fluid. Such model can solve the wave equation for the electric field (and magnetic field, if necessary) at every point in the fluid.

In this study a wave optics model is developed to estimate the optical properties of nanofluids to aid in sizing the absorber tubes and selecting working fluids for directly absorbing solar concentrators. The results computed by the model are compared with those obtained experimentally.

2. Methodology

2.1. Wave Optics Model

The proposed model was constructed using the wave optics module of COMSOL Multiphysics. A 1µm x 1µm x 8µm control volume, figure 1, was defined and given the electrical and optical properties of ethylene glycol. The control volume was large enough to avoid effects resulting from scales close to those of the wavelengths used (diffraction off the edges of the volume) and yet small enough to compute reasonably fast (around 1 hour). The process of simulating the nanoparticles was still complex as the electrical permittivity of a material is governed by the states of charges (protons, electrons) in that material and the amount of the material (Podolskiy et al., 2002). The energy level in which a charge can exist is affected by the number of other charges in the material (Koh et al., 2009).

In bulk samples of material (other than near the edges) the number of surrounding charges approaches infinity (from the perspective of an individual charge) ~~and as such a 10m length of copper will have the same electrical conductivity as 10cm~~. At the nanoscale, however, the number of other charges in a particle is far from infinity (maybe only a couple of thousand) therefore the states available for each individual charge will be different to a charge in a macroscale bulk sample of the same material. Clearly, such bulk measurements for electrical permittivity of a material cannot be used directly for nanoparticles.

This has been observed experimentally by Ni et al. (2007) who reported an apparent difference in refractive index between graphene and graphite of $0.6 - 0.2i$, graphite having a refractive index of $2.6 - 1.3i$ (Palik,1998) and graphene $2.0 - 1.1i$. They attributed this difference to the nano scale of the graphene sheet's thickness.

Within the control volume two arrays were defined comprising identical 5nm x 19nm x 19nm ~~nanoplatelets~~ nanoparticles making up the equivalent of 0.1% of the simulated volume. These ~~nanoplatelets~~ nanoparticles were assigned the complex refractive index of graphene from Ni et al. (2007). The surroundings were assigned the refractive index of ethylene glycol. The arrays were positioned off set from each other so the distance between each particle and a neighbouring particles was not the same, in all directions, see figure 1.

At one of the 1x1 µm faces of the volume a linearly polarised electric field with a power of 25nW (equivalent to a solar radiation intensity of 1000 W/m^2 concentrated 25 times) was applied. The top, bottom and far end faces were assigned impedance boundary conditions while at the other two sides the curl of the magnetic field was set to zero. The model was then used to calculate the electric field at every point in the simulated volume as the electric field at one face was varied from 700nm/428THz to 400nm/750THz in steps of 25THz. The range covered, 700nm/428THz to 400nm/750THz, approximately encompasses the visible solar spectrum (380nm-800nm).

2.2. Experimental investigations

To validate the predictions of the wave optics model experimentally, samples of nanofluids containing ethylene glycol and 5nm x 19nm x 19nm size graphene oxide platelets were prepared via the two step method, where nanoparticles are prepared separately and then added to the base fluid using an ultrasound bath to ensure they are homogenously dispersed. The chosen volume fractions of 0.004%, 0.008%, 0.012%, 0.013%, 0.014% and 0.016% are those over which the absorption is expected to follow a linear trend and are below the critical concentration at which the nanoparticles start to bundle together.

2.2.1. Absorption

The absorption of each sample was measured over the spectrum range of 380nm-800nm in steps of 1nm using Perkin Elmer Lambda 650 S UV/VIS Spectrometer. The instrument was calibrated with a holmium oxide glass standard. A pure sample of ethylene glycol (melting point -12.99 °C and boiling point range 195 - 198 °C at 1,013 hPa) was used as the control. A spectrometer subjects a sample with radiation at a range of wavelengths and measures the intensity of each wavelength passing through it. The disadvantage of this method is that it is more sensitive to low absorbing materials as more radiation are transmitted through them to be measured.

2.2.2. Reflectance

While in the computerized model light enters fluid directly, in the experiment light must first pass through the walls of the fluids container. This will result in four points where the light may be reflected, at each boundary between the air and the container and at the boundaries between the container and the fluid. Any light reflected at these points will not pass through the fluid and will not reach the detector, however it will not have been absorbed by the fluid.

Additionally, light is also scattered within the fluid by the particles. The rationale for the development of the wave optics model was based on the assumption that extinction due to scattering would be low in comparison to extinction resulting from absorption for the nanofluids under investigation as the majority of light scattered within the fluid would still be absorbed before leaving the fluid.

The integrating sphere method is a standard way of measuring the light scattered and reflected by a sample. The instrument is comprised of a sphere, with an inside surface that scatters light evenly around the chamber. When a small part of the surface (referred to as a port) is replaced by a sample, any change in light levels measured by the detector is therefore the result of light scattered back into the chamber by the sample.

The reflectance resulting from the nanofluid samples was measured from 380nm-800nm in steps of 1nm using the same Lambda 650 S UV/VIS in integrating sphere mode. Each sample was placed over an open port and the reflectance was measured by the instrument. For comparison the reflectance of an empty cuvette, a pure sample of ethylene glycol, and the open port were also measured. The light lost by reflection could then be taken from absorbance measurement of each sample to calculate absorption of the fluid sample in isolation.

2.2.3. Stability

To ensure stability of synthesised nanofluids and to confirm repeatability of results, stability tests were carried out on each sample.

Stability is critical for nanofluids to be considered for their use as working fluid in direct solar absorber, if the nanoparticles segregate during periods that the solar concentrator plant is not in use the optical and thermal properties of the nanofluids could be radically altered. Precipitated particles may also block pipes and damage pumps.

To assess the ethylene glycol graphene oxide nanofluid's stability, the 0.008% sample (selected because its absorption had been previously shown to be in the mid-range of the instruments sensitivity) was left undisturbed in the spectrometer. The sample's absorption was measured after 1, 2, 3 and 24 hours to determine the colloidal stability of the fluid over this period. A slight change in the absorption of the sample after 24 hours may be expected as the sample was briefly removed to recalibrate the instrument.

3. Results

3.1 Modelling

The ~~platlets~~ nanoparticles in the simulated volume were assigned the complex refractive indices of Graphene sheets 2.0-1.1i (Ni et al., 2007). The simulated volume with areas of high electric filed strength in red, low electric field strength in blue, is shown in figure 2.

Near the edges of the control volume the boundary conditions force the electric field to be close to zero, as a result smaller control volumes were not penetrated by the electric field. In figure 2 the volume has a cross section measuring 1 µm x 1 µm, which is sufficiently large for the electric field in the centre to propagate mostly unaffected by the boundaries. For each simulation the electric field strength along the x-axis passing through the geometric centroid of the control volume is plotted in figure 3.

While there is substantial variation in the plots there is an overall trend for the field strength to reduce logarithmically with depth, as would be expected from Beer-Lamberts law, equation 2, as shown by the trend line. Initial investigations revealed that a larger and more regular variation resulted from the interaction of radiation with the regular array of nanoparticles; changing either the wavelength or the nanoparticles' arrangement in the array altered this trend. Figure 3 also shows that the properties of the nanoparticles also affected the positions of peaks and troughs.

A smaller scale less regular variation seemed to be resulting from a combination of the mesh and particle shape, the corners of the cuboids had a particularly strong effect on the electric field (figure 4a), and can also be seen as a distinct checkered pattern visible in certain areas of figure 2. The checkered pattern did not appear for spherical nanoparticles in which case the electric field near particles varied less erratically as shown in figure 4b.

The average values for absorbance in the range of 380nm-800nm of 10mm thick layer of nanofluids containing ethylene glycol with 0.004%-0.016% volume fraction graphene nanoparticles were calculated to obtain the trend line shown figure 5. The absorbance of 0.016% was obtained from simulation results whilst for all other volume fractions the absorbance values were approximated from the graphene trend line (figure 3) assuming Beer-Lamberts law to be applicable. Also the test volume may have been too small (8 µm) to fully average the variations shown in figure 2 and figure 3.

3.2. Experimental results

Results of the computer modelling described in section 3.1 and figure 3 confirmed that Beer-Lamberts law held for the nanofluid; the absorbance doubled when the length of the sample was doubled. This was also the case for volume fraction, when the volume fraction was doubled the absorbance proportionally increased.

3.2.1. Absorption

The absorption spectra of nanofluids measured experimentally are shown in figure 6.

As predicted by the model, the nanofluids were close to be equally absorbing over the full range of the spectrum. To compare the predictions of the model with the experimental measurements the average absorbance across the spectrum (380-800 nm) and volume fractions covered were calculated and plotted in figure 7. Error in measurement was observed to be ±7.5%.

As expected the experimental data points in figure 7 follow a linear relationship. While the absorbance for 0.004% and 0.016% volume fraction were close to those predicted by the model

(figure 5) the intermediate volume fractions were found be up to 1AU higher than the predicted absorbance. This could have been because while the model used the refractive index of graphene, the experiments were carried out on a preparation of graphene oxide. Or this could have been the result of some light being reflected from the surface of the fluid resulting in less radiation reaching the sensor than was predicted by the model that did not consider surface effects.

3.2.2. Reflectance

To remove the effect of reflections from the experimental results and compare them to the simulated values the integrating sphere method was used on the Lambda 650 S UV/VIS to measure the reflectance of the samples. This also confirmed the assumption that scattering is low compared to absorption in the nanofluids investigated.

All the nanofluids samples had a lower reflectance value than the pure ethylene glycol. It was found that the reflectance decreased with increasing concentration of graphene oxide nanoparticles reaching a minimum at volume fraction of 0.012%. An increase in the volume fraction beyond 0.012% resulted into a rise in the reflectance as can be seen from figure 8. This optimum volume fraction of 0.012% for minimum reflectance is only valid for the pair of the specific nanoparticle (graphene oxide) and the ethylene glycol used in this study. In practice, even a slight change in the geometry and/or surface characteristics of the nanoparticles should alter this minimal volume fraction significantly.

3.2.3. **Stability**

The stability of ethylene glycol graphene oxide nanofluid was assessed by leaving the 0.008% sample ~~(selected because its absorption had been previously shown to be in the mid-range of the instruments sensitivity)~~ undisturbed in the UV/VIS Spectrometer ~~undisturbed~~ for 24 hours. The sample's absorption was measured after 1, 2, 3 and 24 hours. The change in absorbance measured over the 24-hour time period was negligible as seen from figure 9 indicating that the fluid remained stable throughout the investigation.

4. Conclusions

The concept of using a wave optics model for the absorption of visible solar radiation (380-800nm) by nanofluids was investigated. It is anticipated that such an approach would allow the suitability of a nanofluid for use in a volumetrically absorbing receiver of a concentrating solar collector to be assessed without the need for extensive laboratory tests on each candidate nanofluid. It was shown that even a relatively crude model, covering a control volume with depth only ten times the largest wavelength of 800nm, could predict the solar absorbance of a nanofluid within 1AU of the trends seen in experimental data. In order to keep the cost of nanofluid low, an optimum volume fraction of 0.012% of graphene oxide is proposed to achieve a minimum reflectance and a sufficiently high absorption for a receiver of 10 mm diameter over the visible spectral range for a solar concentrator with a concentration ratio of 25. This optimum proportion is valid for the graphene oxide-ethylene glycol studied here. The model more accurately predicted the absorbance of the higher volume fraction samples than the lower ones. It is anticipated that a larger control volume will allow lower volume fractions to be simulated directly and so improve the accuracy of the model.

The model was dependant on measurements of refractive index or electrical permittivity of nanometre scale materials as such data is not readily available in peer reviewed public domain. The refractive index of graphene was used in the model to produce predictions that were compared to experimental data gathered on graphene oxide, another potential source of uncertainty in the

results. It is hoped that more research into the properties of nano scale materials will widen the scope and improve the accuracy of wave optics models. Until such data is more widely available, models like the one presented here could reduce the number of laboratory tests needed to select a nanofluid for directly absorbing solar thermal applications as from only one test of the refractive index of a nanoparticle, the properties of those particles in any fluid can be predicted.

Acknowledgements

Authors, Rose, Singh, Tassou, Suresh and Anathraman, thankfully acknowledge the UKIERI-DST grant (IND/CONT/E/14-15/381) which made this research possible.

References

Berg, M.J., Sorensen, C.M. and Chakrabarti A. 2008. Extinction and the optical theorem. Part I. Single particles. JOSA A. 25 (7), 1504-1513.

Bohren, C. F., Huffman, D. R. 1983. Absorption and scattering of light by small particles. John Wiley & Sons.

Gorji, T.B. and Ranjbar, A.A., 2015. Geometry optimization of a nanofluid-based direct absorption solar collector using response surface methodology. Solar Energy 122, 314-325.

Hill, J.M. and Jennings, M.J., 1993. Formulation of model equations for heating by microwave radiation. Applied mathematical modelling 17(7), 369-379.

Jain, P.K., Kyeong S.L., Ivan H. and El-Sayed, M.A., 2006. Calculated absorption and scattering properties of gold nanoparticles of different size, shape, and composition: applications in biological imaging and biomedicine. The Journal of Physical Chemistry B 110 (14), 7238-7248.

Kerker, M.P., McNulty, P.J., Sculley, M., Chew, H. and Cooke, D.D., 1978. Raman and fluorescent scattering by molecules embedded in small particles: numerical results for incoherent optical processes. JOSA 68(12), 1676-1686.

Kong, Y. and Cha, C.Y., 1996. Reduction of NOx adsorbed on char with microwave energy. Carbon, 34(8), 1035-1040.

Kottmann, J., Olivier, M., Smith, D. and Schultz,S.. 2000. Spectral response of plasmon resonant nanoparticles with a non-regular shape. Optics express 6 (11), 213-219.

Ladjevardi, S.M., Asnaghi, A., Izadkhast, P.S. and Kashani, A.H., 2013. Applicability of graphite nanofluids in direct solar energy absorption. Solar Energy 94, 327-334.

Lance, K.K., Coronado, E., Zhao, L. and Schatz, G.C. 2003. The optical properties of metal nanoparticles: the influence of size, shape, and dielectric environment. The Journal of Physical Chemistry B 107 (3), 668-677.

Leen, K.A., Bao,K., Khan, I., Smith, W.E., Kothleitner, G., Nordlander, P., Maier, S.A. and McComb, D.W. 2009. Electron energy-loss spectroscopy (EELS) of surface plasmons in single silver nanoparticles and dimers: influence of beam damage and mapping of dark modes. Acs Nano 3 (10), 3015-3022.

Maikala R.V., 2010, Modified Beer's Law – historical perspectives and relevance in near-infrared monitoring of optical properties of human tissue. International Journal of Industrial Ergonomics, 40, 125-134.

Ni, Z.H., Wang, H.M., Kasim, J., Fan, H.M., Yu, T., Wu, Y.H., Feng, Y.P. and Shen, Z.X., 2007. Graphene thickness determination using reflection and contrast spectroscopy. Nano letters 7(9), 2758-2763.

Novotny, L., Hecht, B. 2006. Principles of Nano-Optics. Cambridge University Press.

Otanicar, T.P., Phelan, P.E. and Golden, J.S., 2009. Optical properties of liquids for direct absorption solar thermal energy systems. Solar Energy, 83(7), 969-977.

Palik, E.D., 1998. Handbook of optical constants of solids (Vol. 3). Academic press.

Parameshwaran, R., Jayavel, R., and Kalaiselvam, S. 2013. Study on thermal properties of organic ester phase-change material embedded with silver nanoparticles. Journal of thermal analysis and calorimetry, 114(2), 845-858.

Peatross, J. and Ware, M., 2011. Physics of light and optics (pp. 101-119). Brigham Young University, Department of Physics.

Podolskiy, V.A., Sarychev, A.K. and Shalaev, V.M. 2002. Plasmon modes in metal nanowires and left-handed materials. Journal of Nonlinear Optical Physics & Materials 11 (1), 65-74.

Romasanta, L.J., Hernández, M., López-Manchado, M.A. and Verdejo, R., 2011. Functionalised graphene sheets as effective high dielectric constant fillers. Nanoscale research letters 6(1), 1-6.

Taylor, R.A., Phelan, P.E., Otanicar, T.P., Adrian, R. and Prasher, R., 2011. Nanofluid optical property characterization: towards efficient direct absorption solar collectors. Nanoscale research letters 6(1), 1-11.

Toppin-Hector A., Singh H., 2013, Development of a nano-heat transfer fluid cooled direct absorbing receiver for concentrating solar collectors. Int. J. Low Carbon Technologies 0, 1-6.

Investigations into nanofluids as direct solar radiation collectors

B.A.J. Rose[a] , H. Singh[a*] , N. Verma[a], S. Tassou[a], S. Suresh[b], N. Anantharaman[b], D. Mariotti[c] , P. Maguire[c]

[a]Institute of Energy Futures, Brunel University London, Uxbridge, UB8 3PH, UK
[b]National Institute of Technology, Tiruchirappalli-620015, India
[c]Nanotechnology & Integrated Bio-Engineering Centre, Ulster University, Newtownabbey, BT37 0QB, UK

*Corresponding author (harjit.singh@brunel.ac.uk)

Abstract

Nanofluids that directly absorb solar radiation have been proposed as an alternative to selectively coated metallic receivers in solar thermal collectors. Given the expense of characterising a potential nanofluid experimentally methods for comparing nanofluids virtually are needed. This paper develops a computational wave optics model using COMSOL to simulate the absorption of nanoparticles suspended in a fluid for solar radiation (380-800 nm) and compares it to experimental results using reflectance and transmission spectrometry. It was concluded that while both yielded data with matching trends, the exact absorption of some fluids differed by up to 1 AU. Optical characteristics of nanofluids comprising ethylene glycol (melting point -12.99 °C and boiling point range 195 - 198 °C at 1,013 hPa) and graphene oxide (sheets size 5nm x 19nm x 19nm, volume fraction 0.004-0.016%) have been experimentally measured. An optimum volume fraction of 0.012% of graphene oxide has been identified achieving a minimum reflectance and highest absorbance over the visible spectral range.

Keywords: Nanofluid, Direct solar absorption, Solar thermal collector, Optical absorption, Nanofluid stability, Wave optics model

Highlights

- Different modelling approaches for the direct absorption of solar radiation by nanofluids discussed and evaluated.
- A wave optics model proposed for direct solar absorbing nanofluids.
- The wave optics model constructed and the results analysed.
- The optical properties of graphene oxide-ethylene glycol nanofluids characterised experimentally.
- The experimental results compared to those predicted by the model.

1. Introduction

Nanofluids, suspensions of nanoparticles in liquids, have been the focus of recent interest for use as directly absorbing working fluids, due to their reported stability in suspension and the availability of materials from which they can be synthesised (Romasanta et al., 2011). Directly absorbing nanofluids offer many advantages over traditional surface absorbers: reduced thermal and radiative

losses, potential for miniaturisation of solar concentrators and lower material costs (Toppin-Hector and Singh, 2013). The amount of solar radiation that a solar concentrator working fluid will directly absorb depends primarily on the type of fluid used and its solar absorption characteristics and the dimensions of the receiver tube (Gorji and Ranjbar, 2015; Toppin-Hector and Singh, 2013).

Extinction describes the reduction in the amount of radiation that is observed when any medium (gas or liquid or solid or a combination) is placed between a light source and a detector (Otanicar et al., 2009).

The attenuation of light intensity ($-dI_x$) as light passes through a layer of an absorbing medium is proportional to the intensity of light at the entrance of the medium layer (I_x) and the differential thickness of the layer (dx). Mathematically this relation can be expressed as (Maikala, 2010):

$$-dI_x = aI_x\, dx \tag{1}$$

Where

a is the wavelength dependent absorption or extinction coefficient

Equation (1) is popularly known as Bouguer-Lambert's law and in this equation '–' sign indicates a definite decrease in the intensity as light passes through any absorbing medium.

Previous studies have focussed on the scattering component using an adaptation of the Rayleigh approximation (Ladjevardi et al., 2013). However, the Rayleigh approximation only holds for particles that are spherical, are close in refractive index to the medium they are in, and are small in size relative to the wavelength (λ) such that $\ll \lambda/10$ (Kerker et al., 1978). Models based on the Rayleigh approximation will not be able to predict the optical properties of non-spherical particles such as graphene nanoparticles.

Taylor et al. (2011) took a Maxwell-Garnett effective medium approach to model the optical properties of nanofluids based on the optical properties of the fluid and the bulk materials of the nanoparticles (NPs). Their study has a serious drawback in that they did not consider any difference in the electrical permittivity between a nano scale particle and a macro scale sample of the same metal. They concluded that the Maxwell-Garnett effective medium approach did not correctly predict the extinction caused by nanoparticles in a fluid but did not expand on the reason nor suggest alternative methods.

Beer-Lambert's law relates the reduction in the intensity of light with the depth of medium layer as it passes through an absorbing medium of a specific concentration (C). Thus equation (1) can be expressed as equation (2) as follows:

$$-dI_x = aI_xC\, dx \tag{2}$$

Equation (2) can be integrated over the thickness of the medium layer varying from $x = 0$ to $x = L$ to yield Beer's law (Maikala, 2010):

$$A = log_{10}\frac{I_o}{I} \tag{3}$$

Where

A is the absorbance of the absorbing medium

I_0 is the intensity of light that enters the medium

I is the intensity of light that leaves the medium layer of thickness L

Absorbance therefore can be easily linked with the depth of a medium. Beer-Lamberts law allows the absorbance for any path length through a medium to be calculated. This principle can be interpreted so that it is only necessary for a model to simulate the optical properties of a small volume of fluid to be useful for predicting the absorption of any volume. Currently the optical properties of each different fluid and particle combination must be measured experimentally to identify the ideal working fluid for a direct solar absorption application. If a computer model could be developed that is capable of identifying the most likely nanoparticle-fluid combinations, the process of designing a directly absorbing solar thermal concentrator would be greatly simplified.

1.1. Modelling approach

1.1.1. Raytracing

One of the simplest ways to model light absorption by objects is ray tracing. Ray tracing models light as being composed of several (how many depends on the precision of the model) infinitely narrow straight rays. A nanofluid would be simulated by a ray trace model as a series of opaque objects randomly distributed throughout a transparent medium (the population density and size of the objects is analogous to the volume fraction and size of nanoparticles). Rays are then passed through the virtual nanofluid and when they are incident on a nanoparticle they are considered to have been absorbed and propagate no further by simpler models. Once every incident ray has encountered a sphere and been absorbed, the distance travelled by the last ray to be absorbed and the number of rays used in the simulation can be used to estimate the depth of the fluid layer to cause full absorption of the solar radiation.

Ray trace models have the advantage of requiring relatively little information about the nanofluids and are based on simple geometric calculations to produce a result. However, they cannot accurately simulate the absorption of solar radiation by nanofluids as nanoparticles are significantly smaller than the wavelength of solar radiation.

The uncertainty in the position of a photon makes it difficult to determine if a photon will be absorbed by a nanoparticle using a ray trace model. For a photon, it can be derived from the uncertainty principle expressed in equation (4).

$$\Delta x \geq \frac{\lambda}{4\pi} \tag{4}$$

where (Δx) is the uncertainty in position and (λ) is the wavelength.

For a photon of visible light uncertainty in the position is always greater than $\sim$40nm which is larger than the size of many nanoparticles considered for direct absorption (size $\sim 15-30$nm). As such modelling light as rays at scales less than this is not a meaningful analogy (Novotny, 2006). The wavelength of visible light could easily be around 10-25 times greater than the size of NPs. Thus, model assumption that light travels in straight lines and is only absorbed by particles on which it is directly incident is not valid (Bohen, 1983).

As a result of these two shortcomings, a purely ray tracing based model only considers the interaction between particles and light directly incident on it. Such a model would either under- or over-estimate the optical absorption by a nanofluid. An alternative would therefore be to simulate the process using ray tracing only at scales where its assumptions are sensible and an alternative model to simulate the fluid properties at smaller scales.

1.1.2. Wave optics

While the Rayleigh approximation was originally derived geometrically it has been shown to be consistent with wave optics (Bohren and Huffman, 1983).

The interaction of electric and magnetic fields is described physically by Maxwell's, equations (5)-(8).

$$\nabla \times \boldsymbol{E}(\boldsymbol{r},t) = -\frac{\partial \boldsymbol{B}(\boldsymbol{r},t)}{\partial t} \quad (5)$$

$$\nabla \times \boldsymbol{H}(\boldsymbol{r},t) = \frac{\partial \boldsymbol{D}(\boldsymbol{r},t)}{\partial t} + \boldsymbol{j}(\boldsymbol{r},t) \quad (6)$$

$$\nabla . \boldsymbol{D}(\boldsymbol{r},t) = \rho(\boldsymbol{r},t) \quad (7)$$

$$\nabla . \boldsymbol{B}(\boldsymbol{r},t) = 0 \quad (8)$$

Where (E) is the electric field; (D) is the electric displacement; (H) is the magnetic field; (B) is the magnetic induction; (j) is the current density, (ρ) is the charge density, $(\nabla \times)$ represents the curl of a vector and $(\nabla .)$ represents the divergence of the vector.

Light is therefore described by wave optics as an electromagnetic wave comprised of varying electric and magnetic fields orthogonal to each other and the direction of wave propagation.

In vacuum electromagnetic waves will continue to propagate indefinitely whereas in other mediums charges will be affected by the varying electrical and magnetic field which will diminish energy content of the wave as it passes through. In this way the electromagnetic wave is absorbed and its energy is transferred to the medium.

A medium's resistance to a change in electric field and magnetic field is given by the electrical permittivity (ε) and magnetic permeability (μ) respectively. These properties are more commonly represented in terms of the refractive index (n) (9).

$$n = \sqrt{\frac{\varepsilon}{\varepsilon_0}\frac{\mu}{\mu_0}} \quad (9)$$

Where (ε_0) is the electrical permittivity of free space and (μ_0) is the magnetic permeability of free space.

In most circumstances, at speeds much less than the speed of light or intensities less than 10^{18} W/m^2, only the electric field and electrical permittivity need be considered (Peatross, and Ware, 2011). The wave equation for the electric field in a medium with a refractive index (n) can be written as shown in equation (10).

$$\nabla^2 E - \frac{n^2}{c^2}\frac{\partial^2 E}{\partial t^2} = 0 \quad (10)$$

Where (c) is the speed of light.

A wave optics model of a nanofluid can be built from the refractive indices of the nanoparticles and base fluid, particle size and particle distribution in the fluid. Such model can solve the wave equation for the electric field (and magnetic field, if necessary) at every point in the fluid.

In this study a wave optics model is developed to estimate the optical properties of nanofluids to aid in sizing the absorber tubes and selecting working fluids for directly absorbing solar concentrators. The results computed by the model are compared with those obtained experimentally.

2. Methodology

2.1. Wave Optics Model

The proposed model was constructed using the wave optics module of COMSOL Multiphysics. A 1µm x 1µm x 8µm control volume, figure 1, was defined and given the electrical and optical properties of ethylene glycol. The control volume was large enough to avoid effects resulting from scales close to those of the wavelengths used (diffraction off the edges of the volume) and yet small enough to compute reasonably fast (around 1 hour). The process of simulating the nanoparticles was still complex as the electrical permittivity of a material is governed by the states of charges (protons, electrons) in that material and the amount of the material (Podolskiy et al., 2002). The energy level in which a charge can exist is affected by the number of other charges in the material (Koh et al., 2009).

In bulk samples of material (other than near the edges) the number of surrounding charges approaches infinity (from the perspective of an individual charge). At the nanoscale, however, the number of other charges in a particle is far from infinity (maybe only a couple of thousand) therefore the states available for each individual charge will be different to a charge in a macroscale bulk sample of the same material. Clearly, such bulk measurements for electrical permittivity of a material cannot be used directly for nanoparticles.

This has been observed experimentally by Ni et al. (2007) who reported an apparent difference in refractive index between graphene and graphite of $0.6 - 0.2i$, graphite having a refractive index of $2.6 - 1.3i$ (Palik,1998) and graphene $2.0 - 1.1i.$ They attributed this difference to the nano scale of the graphene sheet's thickness.

Within the control volume two arrays were defined comprising identical 5nm x 19nm x 19nm nanoparticles making up the equivalent of 0.1% of the simulated volume. These nanoparticles were assigned the complex refractive index of graphene from Ni et al. (2007). The surroundings were assigned the refractive index of ethylene glycol. The arrays were positioned off set from each other so the distance between each particle and a neighbouring particles was not the same, in all directions, see figure 1.

At one of the 1x1 µm faces of the volume a linearly polarised electric field with a power of 25nW (equivalent to a solar radiation intensity of 1000 W/m^2 concentrated 25 times) was applied. The top, bottom and far end faces were assigned impedance boundary conditions while at the other two sides the curl of the magnetic field was set to zero. The model was then used to calculate the electric field at every point in the simulated volume as the electric field at one face was varied from 700nm/428THz to 400nm/750THz in steps of 25THz. The range covered, 700nm/428THz to 400nm/750THz, approximately encompasses the visible solar spectrum (380nm-800nm).

2.2. Experimental investigations

To validate the predictions of the wave optics model experimentally, samples of nanofluids containing ethylene glycol and 5nm x 19nm x 19nm size graphene oxide platelets were prepared via the two step method, where nanoparticles are prepared separately and then added to the base fluid using an ultrasound bath to ensure they are homogenously dispersed. The chosen volume fractions of 0.004%, 0.008%, 0.012%, 0.013%, 0.014% and 0.016% are those over which the absorption is expected to follow a linear trend and are below the critical concentration at which the nanoparticles start to bundle together.

2.2.1. Absorption

The absorption of each sample was measured over the spectrum range of 380nm-800nm in steps of 1nm using Perkin Elmer Lambda 650 S UV/VIS Spectrometer. The instrument was calibrated with a holmium oxide glass standard. A pure sample of ethylene glycol (melting point -12.99 °C and boiling point range 195 - 198 °C at 1,013 hPa) was used as the control. A spectrometer subjects a sample with radiation at a range of wavelengths and measures the intensity of each wavelength passing through it. The disadvantage of this method is that it is more sensitive to low absorbing materials as more radiation are transmitted through them to be measured.

2.2.2. Reflectance

While in the computerized model light enters fluid directly, in the experiment light must first pass through the walls of the fluids container. This will result in four points where the light may be reflected, at each boundary between the air and the container and at the boundaries between the container and the fluid. Any light reflected at these points will not pass through the fluid and will not reach the detector, however it will not have been absorbed by the fluid.

Additionally, light is also scattered within the fluid by the particles. The rationale for the development of the wave optics model was based on the assumption that extinction due to scattering would be low in comparison to extinction resulting from absorption for the nanofluids under investigation as the majority of light scattered within the fluid would still be absorbed before leaving the fluid.

The integrating sphere method is a standard way of measuring the light scattered and reflected by a sample. The instrument is comprised of a sphere, with an inside surface that scatters light evenly around the chamber. When a small part of the surface (referred to as a port) is replaced by a sample, any change in light levels measured by the detector is therefore the result of light scattered back into the chamber by the sample.

The reflectance resulting from the nanofluid samples was measured from 380nm-800nm in steps of 1nm using the same Lambda 650 S UV/VIS in integrating sphere mode. Each sample was placed over an open port and the reflectance was measured by the instrument. For comparison the reflectance of an empty cuvette, a pure sample of ethylene glycol, and the open port were also measured. The light lost by reflection could then be taken from absorbance measurement of each sample to calculate absorption of the fluid sample in isolation.

2.2.3. Stability

To ensure stability of synthesised nanofluids and to confirm repeatability of results, stability tests were carried out on each sample.

Stability is critical for nanofluids to be considered for their use as working fluid in direct solar absorber, if the nanoparticles segregate during periods that the solar concentrator plant is not in use the optical and thermal properties of the nanofluids could be radically altered. Precipitated particles may also block pipes and damage pumps.

To assess the ethylene glycol graphene oxide nanofluid's stability, the 0.008% sample (selected because its absorption had been previously shown to be in the mid-range of the instruments sensitivity) was left undisturbed in the spectrometer. The sample's absorption was measured after 1, 2, 3 and 24 hours to determine the colloidal stability of the fluid over this period. A slight change in the absorption of the sample after 24 hours may be expected as the sample was briefly removed to recalibrate the instrument.

3. Results

3.1 Modelling

The nanoparticles in the simulated volume were assigned the complex refractive indices of Graphene sheets 2.0-1.1i (Ni et al., 2007). The simulated volume with areas of high electric filed strength in red, low electric field strength in blue, is shown in figure 2.

Near the edges of the control volume the boundary conditions force the electric field to be close to zero, as a result smaller control volumes were not penetrated by the electric field. In figure 2 the volume has a cross section measuring 1 μm x 1 μm, which is sufficiently large for the electric field in the centre to propagate mostly unaffected by the boundaries. For each simulation the electric field strength along the x-axis passing through the geometric centroid of the control volume is plotted in figure 3.

While there is substantial variation in the plots there is an overall trend for the field strength to reduce logarithmically with depth, as would be expected from Beer-Lamberts law, equation 2, as shown by the trend line. Initial investigations revealed that a larger and more regular variation resulted from the interaction of radiation with the regular array of nanoparticles; changing either the wavelength or the nanoparticles' arrangement in the array altered this trend. Figure 3 also shows that the properties of the nanoparticles also affected the positions of peaks and troughs.

A smaller scale less regular variation seemed to be resulting from a combination of the mesh and particle shape, the corners of the cuboids had a particularly strong effect on the electric field (figure 4a), and can also be seen as a distinct checkered pattern visible in certain areas of figure 2. The checkered pattern did not appear for spherical nanoparticles in which case the electric field near particles varied less erratically as shown in figure 4b.

The average values for absorbance in the range of 380nm-800nm of 10mm thick layer of nanofluids containing ethylene glycol with 0.004%-0.016% volume fraction graphene nanoparticles were calculated to obtain the trend line shown figure 5. The absorbance of 0.016% was obtained from simulation results whilst for all other volume fractions the absorbance values were approximated from the graphene trend line (figure 3) assuming Beer-Lamberts law to be applicable. Also the test volume may have been too small (8 μm) to fully average the variations shown in figure 2 and figure 3.

3.2. Experimental results

Results of the computer modelling described in section 3.1 and figure 3 confirmed that Beer-Lamberts law held for the nanofluid; the absorbance doubled when the length of the sample was doubled. This was also the case for volume fraction, when the volume fraction was doubled the absorbance proportionally increased.

3.2.1. Absorption

The absorption spectra of nanofluids measured experimentally are shown in figure 6.

As predicted by the model, the nanofluids were close to be equally absorbing over the full range of the spectrum. To compare the predictions of the model with the experimental measurements the average absorbance across the spectrum (380-800 nm) and volume fractions covered were calculated and plotted in figure 7. Error in measurement was observed to be ±7.5%.

As expected the experimental data points in figure 7 follow a linear relationship. While the absorbance for 0.004% and 0.016% volume fraction were close to those predicted by the model

(figure 5) the intermediate volume fractions were found be up to 1AU higher than the predicted absorbance. This could have been because while the model used the refractive index of graphene, the experiments were carried out on a preparation of graphene oxide. Or this could have been the result of some light being reflected from the surface of the fluid resulting in less radiation reaching the sensor than was predicted by the model that did not consider surface effects.

3.2.2. Reflectance

To remove the effect of reflections from the experimental results and compare them to the simulated values the integrating sphere method was used on the Lambda 650 S UV/VIS to measure the reflectance of the samples. This also confirmed the assumption that scattering is low compared to absorption in the nanofluids investigated.

All the nanofluids samples had a lower reflectance value than the pure ethylene glycol. It was found that the reflectance decreased with increasing concentration of graphene oxide nanoparticles reaching a minimum at volume fraction of 0.012%. An increase in the volume fraction beyond 0.012% resulted into a rise in the reflectance as can be seen from figure 8. This optimum volume fraction of 0.012% for minimum reflectance is only valid for the pair of the specific nanoparticle (graphene oxide) and the ethylene glycol used in this study. In practice, even a slight change in the geometry and/or surface characteristics of the nanoparticles should alter this minimal volume fraction significantly.

3.2.3. **Stability**

The stability of ethylene glycol graphene oxide nanofluid was assessed by leaving the 0.008% sample undisturbed in the UV/VIS Spectrometer for 24 hours. The sample's absorption was measured after 1, 2, 3 and 24 hours. The change in absorbance measured over the 24-hour time period was negligible as seen from figure 9 indicating that the fluid remained stable throughout the investigation.

4. Conclusions

The concept of using a wave optics model for the absorption of visible solar radiation (380-800nm) by nanofluids was investigated. It is anticipated that such an approach would allow the suitability of a nanofluid for use in a volumetrically absorbing receiver of a concentrating solar collector to be assessed without the need for extensive laboratory tests on each candidate nanofluid. It was shown that even a relatively crude model, covering a control volume with depth only ten times the largest wavelength of 800nm, could predict the solar absorbance of a nanofluid within 1AU of the trends seen in experimental data. In order to keep the cost of nanofluid low, an optimum volume fraction of 0.012% of graphene oxide is proposed to achieve a minimum reflectance and a sufficiently high absorption for a receiver of 10 mm diameter over the visible spectral range for a solar concentrator with a concentration ratio of 25. This optimum proportion is valid for the graphene oxide-ethylene glycol studied here. The model more accurately predicted the absorbance of the higher volume fraction samples than the lower ones. It is anticipated that a larger control volume will allow lower volume fractions to be simulated directly and so improve the accuracy of the model.

The model was dependant on measurements of refractive index or electrical permittivity of nanometre scale materials as such data is not readily available in peer reviewed public domain. The refractive index of graphene was used in the model to produce predictions that were compared to experimental data gathered on graphene oxide, another potential source of uncertainty in the results. It is hoped that more research into the properties of nano scale materials will widen the

scope and improve the accuracy of wave optics models. Until such data is more widely available, models like the one presented here could reduce the number of laboratory tests needed to select a nanofluid for directly absorbing solar thermal applications as from only one test of the refractive index of a nanoparticle, the properties of those particles in any fluid can be predicted.

Acknowledgements

Authors, Rose, Singh, Tassou, Suresh and Anathraman, thankfully acknowledge the UKIERI-DST grant (IND/CONT/E/14-15/381) which made this research possible.

References

Berg, M.J., Sorensen, C.M. and Chakrabarti A. 2008. Extinction and the optical theorem. Part I. Single particles. JOSA A. 25 (7), 1504-1513.

Bohren, C. F., Huffman, D. R. 1983. Absorption and scattering of light by small particles. John Wiley & Sons.

Gorji, T.B. and Ranjbar, A.A., 2015. Geometry optimization of a nanofluid-based direct absorption solar collector using response surface methodology. Solar Energy 122, 314-325.

Hill, J.M. and Jennings, M.J., 1993. Formulation of model equations for heating by microwave radiation. Applied mathematical modelling 17(7), 369-379.

Jain, P.K., Kyeong S.L., Ivan H. and El-Sayed, M.A., 2006. Calculated absorption and scattering properties of gold nanoparticles of different size, shape, and composition: applications in biological imaging and biomedicine. The Journal of Physical Chemistry B 110 (14), 7238-7248.

Kerker, M.P., McNulty, P.J., Sculley, M., Chew, H. and Cooke, D.D., 1978. Raman and fluorescent scattering by molecules embedded in small particles: numerical results for incoherent optical processes. JOSA 68(12), 1676-1686.

Kong, Y. and Cha, C.Y., 1996. Reduction of NOx adsorbed on char with microwave energy. Carbon, 34(8), 1035-1040.

Kottmann, J., Olivier, M., Smith, D. and Schultz,S.. 2000. Spectral response of plasmon resonant nanoparticles with a non-regular shape. Optics express 6 (11), 213-219.

Ladjevardi, S.M., Asnaghi, A., Izadkhast, P.S. and Kashani, A.H., 2013. Applicability of graphite nanofluids in direct solar energy absorption. Solar Energy 94, 327-334.

Lance, K.K., Coronado, E., Zhao, L. and Schatz, G.C. 2003. The optical properties of metal nanoparticles: the influence of size, shape, and dielectric environment. The Journal of Physical Chemistry B 107 (3), 668-677.

Leen, K.A., Bao,K., Khan, I., Smith, W.E., Kothleitner, G., Nordlander, P., Maier, S.A. and McComb, D.W. 2009. Electron energy-loss spectroscopy (EELS) of surface plasmons in single silver nanoparticles and dimers: influence of beam damage and mapping of dark modes. Acs Nano 3 (10), 3015-3022.

Maikala R.V., 2010, Modified Beer's Law – historical perspectives and relevance in near-infrared monitoring of optical properties of human tissue. International Journal of Industrial Ergonomics, 40, 125-134.

Ni, Z.H., Wang, H.M., Kasim, J., Fan, H.M., Yu, T., Wu, Y.H., Feng, Y.P. and Shen, Z.X., 2007. Graphene thickness determination using reflection and contrast spectroscopy. Nano letters 7(9), 2758-2763.

Novotny, L., Hecht, B. 2006. Principles of Nano-Optics. Cambridge University Press.

Otanicar, T.P., Phelan, P.E. and Golden, J.S., 2009. Optical properties of liquids for direct absorption solar thermal energy systems. Solar Energy, 83(7), 969-977.

Palik, E.D., 1998. Handbook of optical constants of solids (Vol. 3). Academic press.

Parameshwaran, R., Jayavel, R., and Kalaiselvam, S. 2013. Study on thermal properties of organic ester phase-change material embedded with silver nanoparticles. Journal of thermal analysis and calorimetry, 114(2), 845-858.

Peatross, J. and Ware, M., 2011. Physics of light and optics (pp. 101-119). Brigham Young University, Department of Physics.

Podolskiy, V.A., Sarychev, A.K. and Shalaev, V.M. 2002. Plasmon modes in metal nanowires and left-handed materials. Journal of Nonlinear Optical Physics & Materials 11 (1), 65-74.

Romasanta, L.J., Hernández, M., López-Manchado, M.A. and Verdejo, R., 2011. Functionalised graphene sheets as effective high dielectric constant fillers. Nanoscale research letters 6(1), 1-6.

Taylor, R.A., Phelan, P.E., Otanicar, T.P., Adrian, R. and Prasher, R., 2011. Nanofluid optical property characterization: towards efficient direct absorption solar collectors. Nanoscale research letters 6(1), 1-11.

Toppin-Hector A., Singh H., 2013, Development of a nano-heat transfer fluid cooled direct absorbing receiver for concentrating solar collectors. Int. J. Low Carbon Technologies 0, 1-6.

Highlights

- Different modelling approaches for the direct absorption of solar radiation by nanofluids discussed and evaluated.
- A wave optics model proposed for direct solar absorbing nanofluids.
- The wave optics model constructed and the results analysed.
- The optical properties of graphene oxide-ethylene glycol nanofluids characterised experimentally.
- The experimental results compared to those predicted by the model.

Figure 1

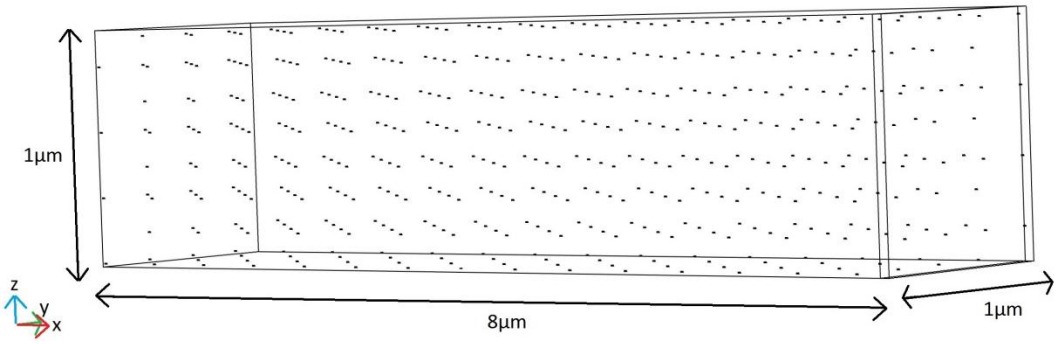

Figure 1. The simulated control volume containing two offset nanoparticle arrays

Figure 2

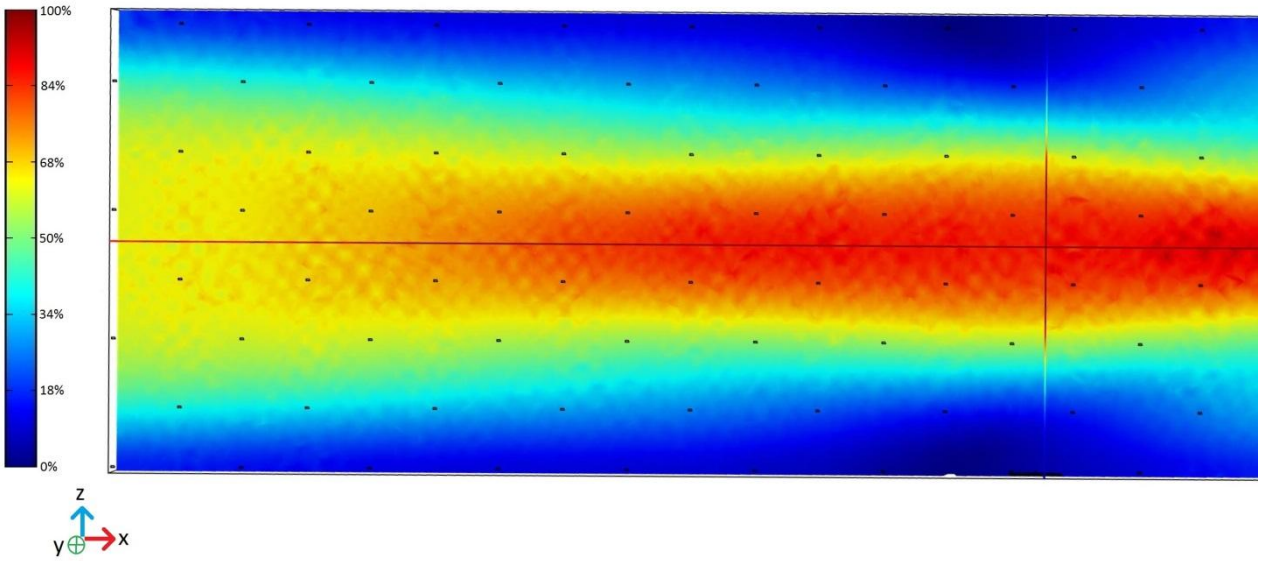

Figure 2. Electric field strength in the simulated volume, the field enters at the right hand side; high electric field strength areas are shown in red and low electric field strength in blue.

Figure 3

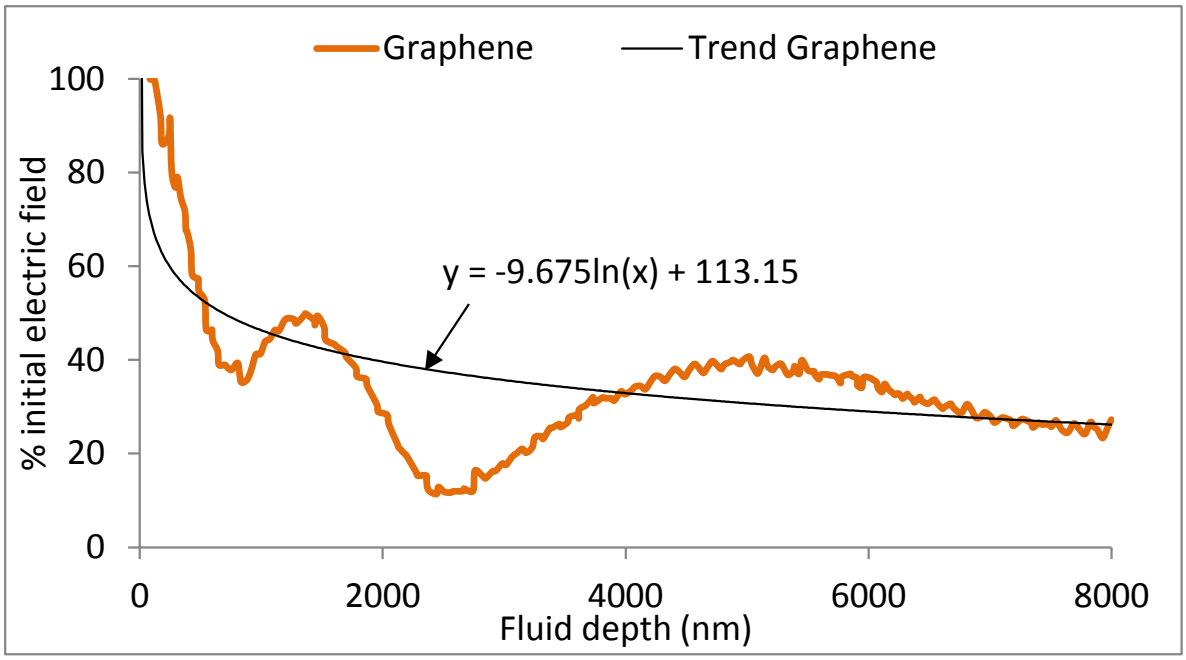

Figure 3. Variation of electric field with depth on the central x-axis of the simulated control volume

Figure 4

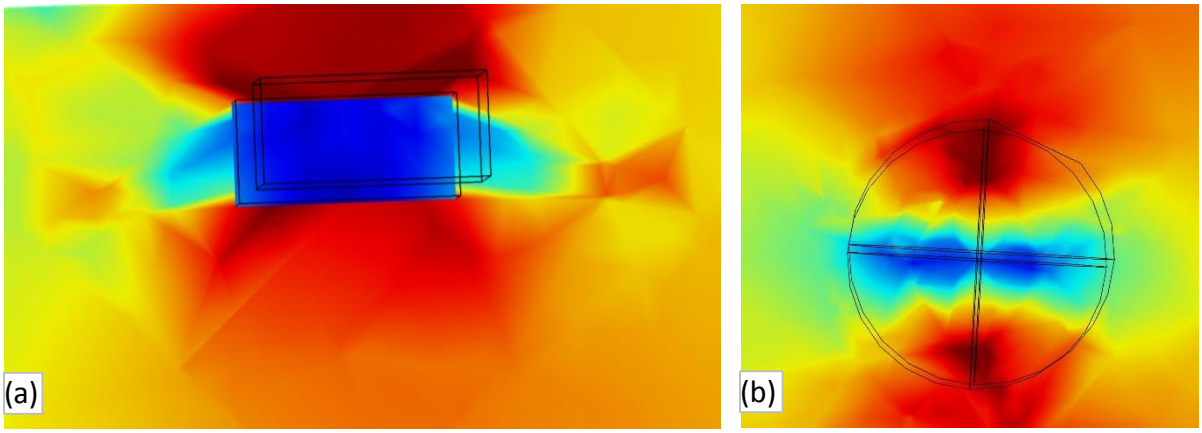

Figure 4. Electric field strength around (a) a cuboid particle and (b) a spherical particle; red areas show a higher electric field strength and blue a low electric field strength

Figure 5

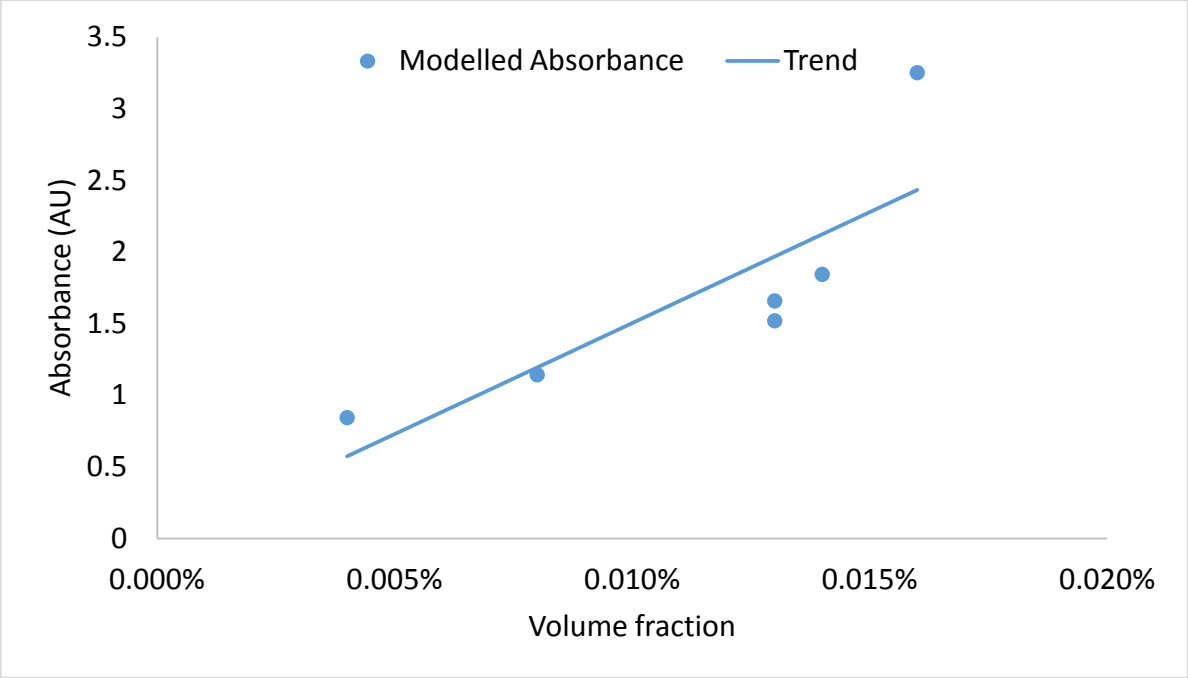

Figure 5. Model predicted absorbance for ethylene glycol and graphene nanofluids

Figure 6

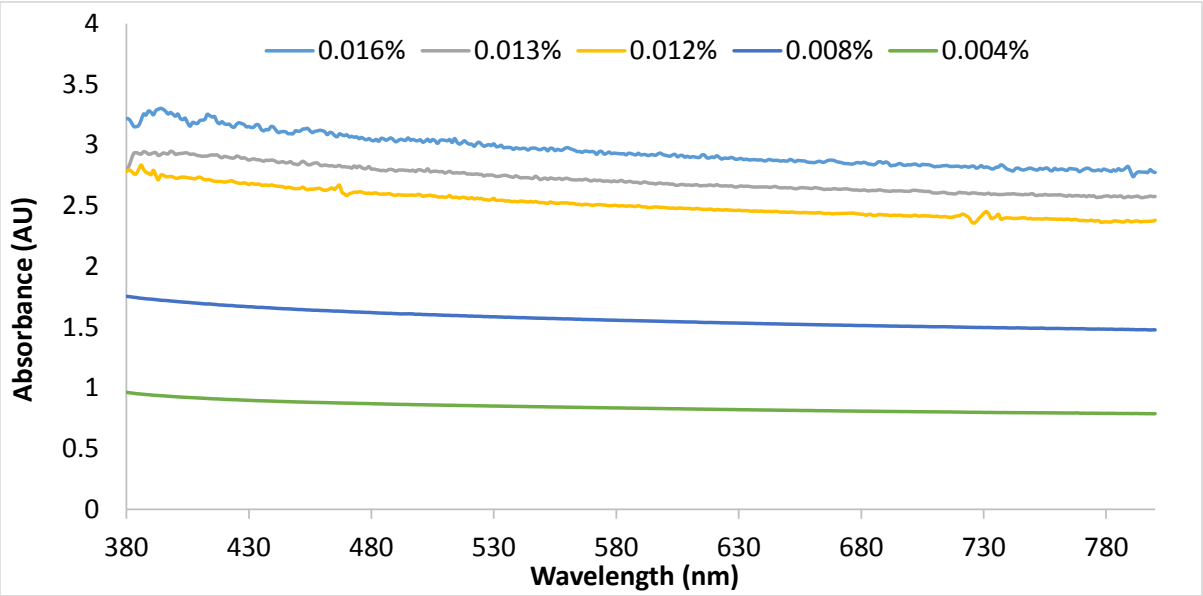

Figure 6. Absorbance spectra of nanofluids with different volume fractions of graphene oxide

Figure 7

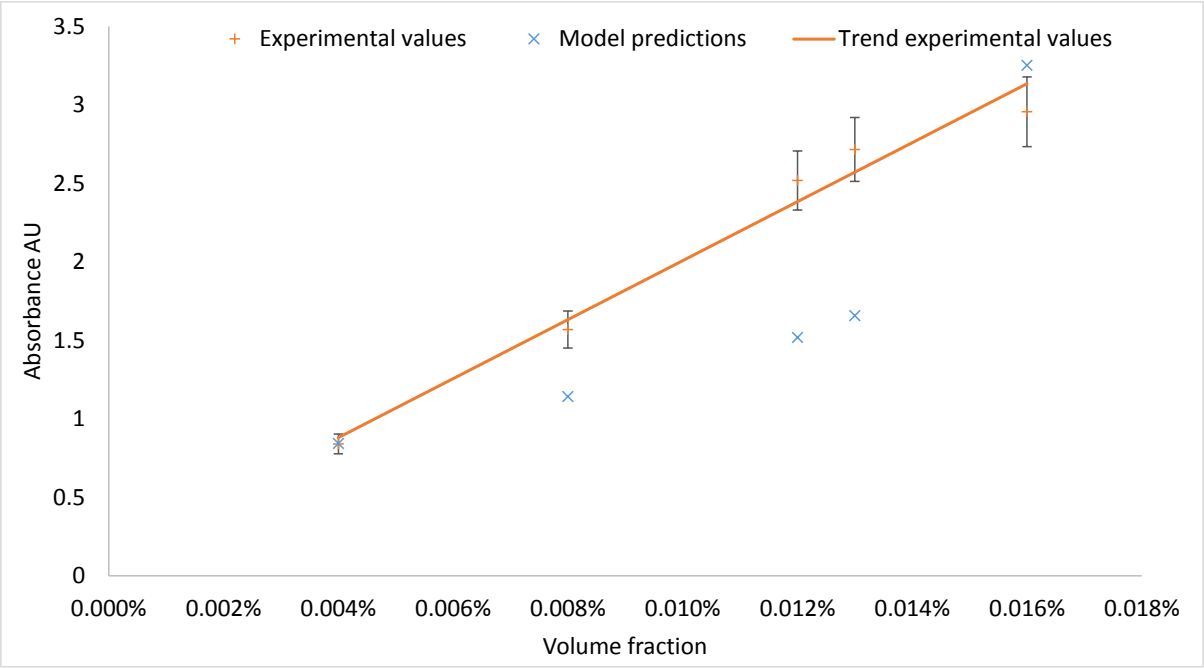

Figure 7. Modelled and experimental average absorbance of nanofluids across the solar spectrum (380-800 nm)

Figure 8

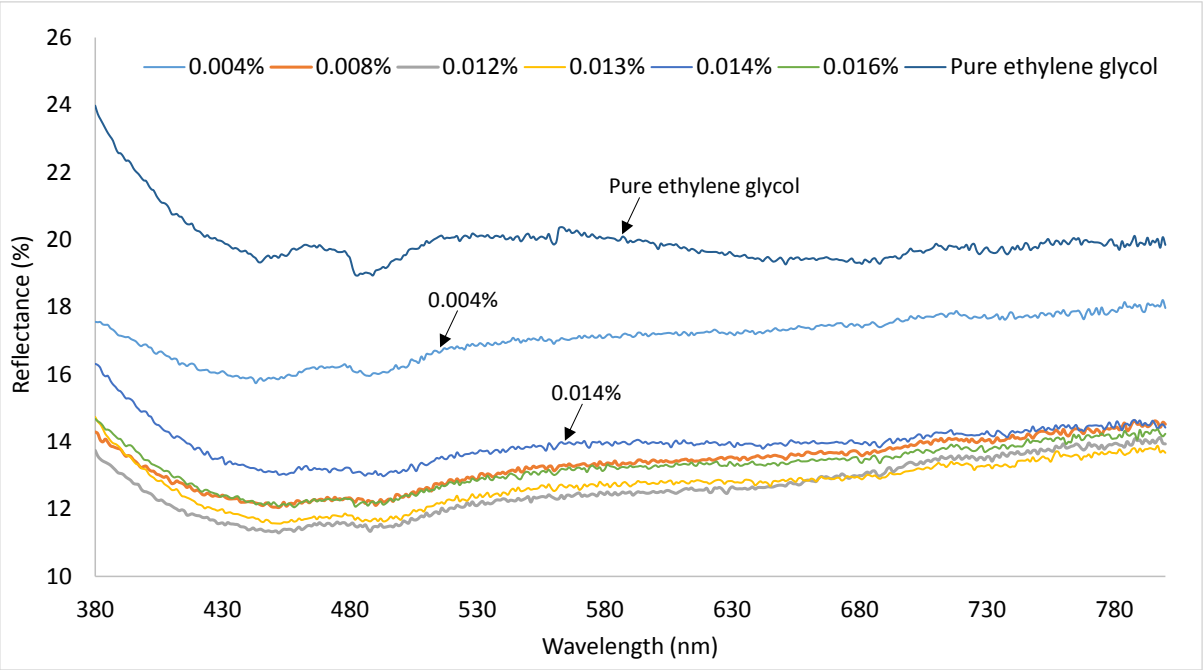

Figure 8. Reflectance spectrum for different volume fractions

Figure 9

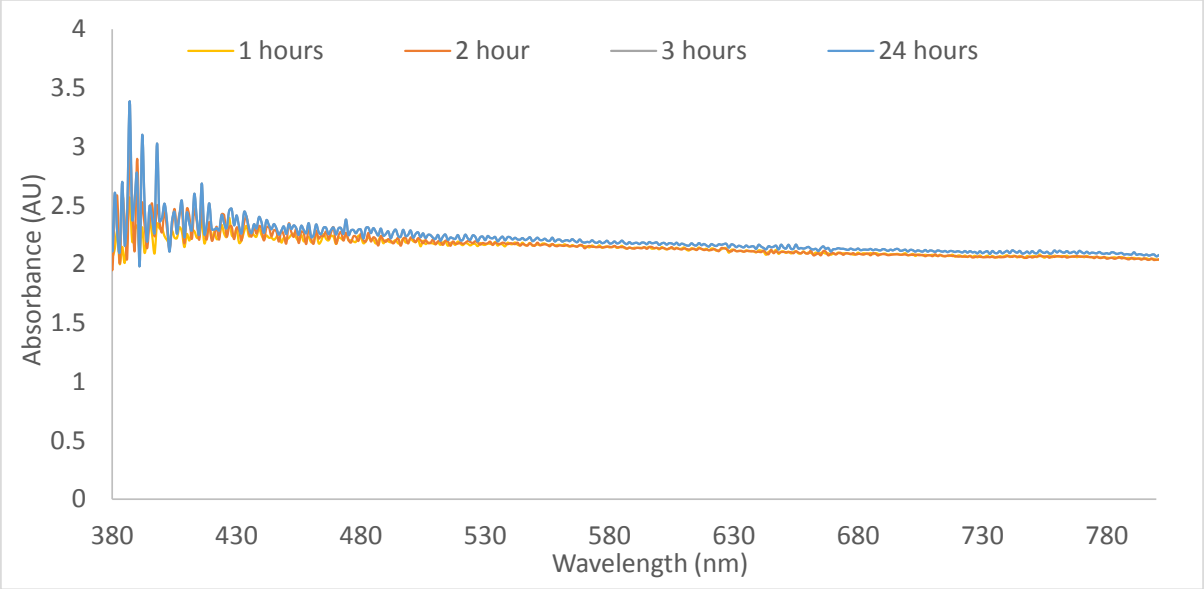

Figure 9. Stability of nanofluid containing ethylene glycol and 0.008% graphene oxide